We are IntechOpen, the world's leading publisher of Open Access books Built by scientists, for scientists

6,900
Open access books available

184,000
International authors and editors

200M
Downloads

Our authors are among the

154
Countries delivered to

TOP 1%
most cited scientists

12.2%
Contributors from top 500 universities



WEB OF SCIENCE™

Selection of our books indexed in the Book Citation Index in Web of Science™ Core Collection (BKCI)

Interested in publishing with us?
Contact book.department@intechopen.com

Numbers displayed above are based on latest data collected.
For more information visit www.intechopen.com



Chapter 4

The Importance of the Fluorine Effect on the Oxidation of Intermetallic Titanium Aluminides

Alexander Georg Donchev and
Mathias Christian Galetz

Additional information is available at the end of the chapter

http://dx.doi.org/10.5772/intechopen.75696

Abstract

Due to the low Al activity within technical titanium aluminides and the similar thermodynamic stabilities of Al- and Ti-oxide these alloys always form a mixed oxide scale at elevated temperatures consisting of TiO_2, Al_2O_3 and also nitrides if the exposure takes place in air. This mixed scale does not provide any oxidation protection especially under thermocyclic load or in water vapor containing environments. Thus accelerated oxidation occurs. Alloying of additional elements such as Nb improves the oxidation behavior if the additions stay within a certain concentration range but such additions cannot suppress non-protective mixed scale formation. Coatings are another way to protect these materials but several obstacles and new degradation mechanisms exist such as delamination e.g. due to CTE mismatch or development of brittle intermetallic phases due to interdiffusion. Therefore, other suitable protective measures have to be undertaken to make sure a protective oxide scale will develop. The so called halogen effect is a very promising way to change the oxidation mechanism from mixed scale formation to alumina formation. After optimized halogen treatment the alumina layer is very protective up to several thousand hours even under thermocyclic load and in atmospheres containing water vapor or SO_2.

Keywords: titanium aluminides, oxidation, halogen effect

1. Introduction

Intermetallics possess very interesting properties due to their unique ordered crystal structure, which differs from those of the constituting elements. Bonding includes metallic and covalent portions so that they combine metallic and ceramic properties such as high strength and decent corrosion resistance but on the other hand usually low ductility at room temperature

IntechOpen

© 2018 The Author(s). Licensee IntechOpen. This chapter is distributed under the terms of the Creative Commons Attribution License (http://creativecommons.org/licenses/by/3.0), which permits unrestricted use, distribution, and reproduction in any medium, provided the original work is properly cited. CC BY

(RT). Some of these materials are promising candidates to replace conventional heavy nickel-based alloys in several high-temperature (HT) applications. In particular, alloys based on titanium and aluminum, so-called titanium aluminides, consisting predominantly of the γ-TiAl phase have a high service potential (**Figure 1**). Their density is only about 4 g/cm^3, which is about half that of conventional Ni-based superalloys. The specific strength of this new class of materials is even higher than that of Ni alloys [1]. Technical TiAl alloys have an Al content of about 40–50 at.% and consist of at least two phases, i.e., γ-TiAl and α_2-Ti_3Al. Recent developments have led to alloys with an Al content below 45 at.% and additions of β-stabilizing elements such as Nb or Mo, which solidify via the β-phase to have three phases α_2, γ, and β_0 present at service temperature [2]. All in all the average composition of such technical TiAl alloys can be written as Ti (42–48), Al (2–8), Nb (0.5–3), other metals such as Cr or Mo (0.1–1), and nonmetals as B, C, and Si (0.1–0.5) [3].

Still, there are some drawbacks to the widespread distribution of titanium aluminides, i.e., low room temperature ductility [4] and low oxidation resistance at temperatures above ca. 750°C [5], which are major topics in research all over the world. Alloying of additional elements can improve the oxidation resistance [6] but is usually not sufficient to lift the application temperature far above the current range of application up to 750°C.

Due to the similar thermodynamic stabilities of Al and Ti oxide and an Al activity too low to form Al_2O_3, these alloys always develop a mixed oxide scale at elevated temperatures in oxidizing environments [7]. The scale consists of TiO_2, Al_2O_3, and also nitrides if the exposure

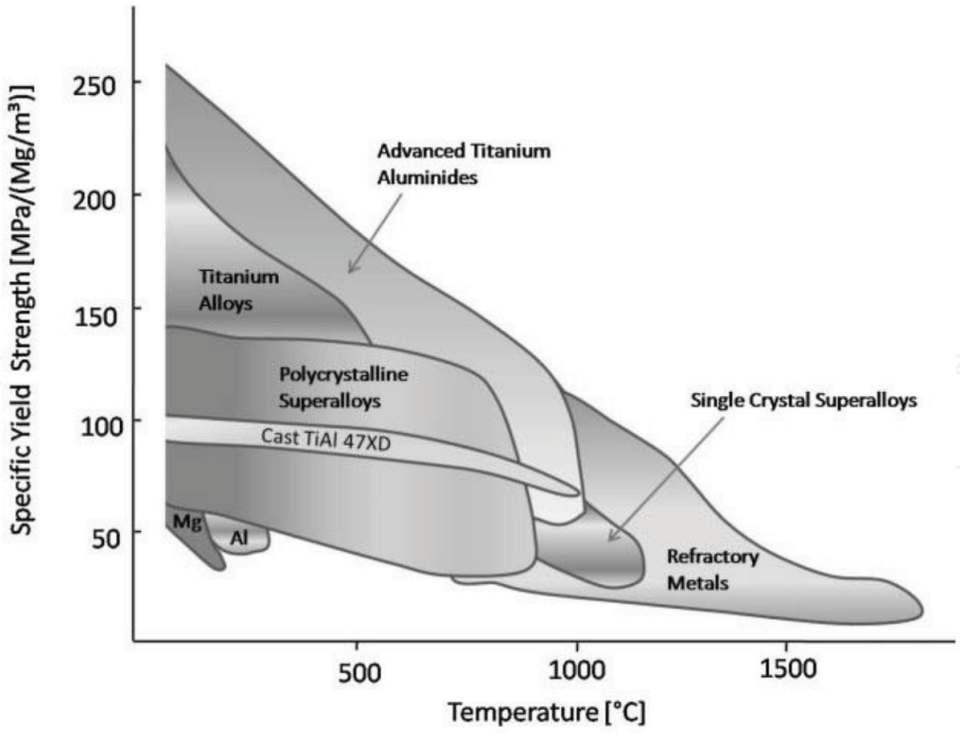


Figure 1. Comparison of the specific yield strength of engineering materials, which are used in automotive engines and in aeroengines. The figure shows that advanced titanium aluminide alloys are capable to bear higher application temperatures and loads than Ti alloys. It is evident that TiAl alloys have an advantage over Ti-based materials [1].

http://dx.doi.org/10.5772/intechopen.75696

takes place in air [8]. TiO_2 grows very fast at temperatures above 600°C so that the mixed scales can get very thick within rather short exposure times. The mixed scale does not provide oxidation protection especially under thermal cyclic load. Due to the different coefficient of thermal expansion (CTE) of the substrate and the oxides, stresses arise which can lead to spallation of the scale if a certain stress level is reached [9]. This can happen especially during cooling down from service temperature. Thus, accelerated oxidation will occur. Alloying of additional elements such as Nb improves the oxidation behavior if the additions stay within a certain concentration range, but all these additions cannot suppress the mixed scale formation [6]. Coatings are another way to protect these materials, but several obstacles and new degradation mechanisms exist such as delamination, e.g., due to CTE mismatch or development of brittle intermetallic phases due to interdiffusion [5]. Therefore, other suitable protective measures have to be undertaken to make sure a protective oxide scale will develop. The so-called halogen effect is a very promising way to change the oxidation mechanism from mixed scale formation to alumina formation. After optimized halogen treatment, the alumina layer is very protective up to several thousand hours even under thermolcyclic load and in atmospheres containing water vapor or SO_2 [10].

2. Mechanism

Due to alumina formation by the halogen effect, the oxidation kinetics of halogenated specimens is reduced compared to that of untreated TiAl. In **Figure 2** the mass change data derived from thermogravimetric analysis, i.e., mass change measuring during isothermal oxidation, are shown. The mass change curve of the fluorinated sample reveals the beneficial fluorine

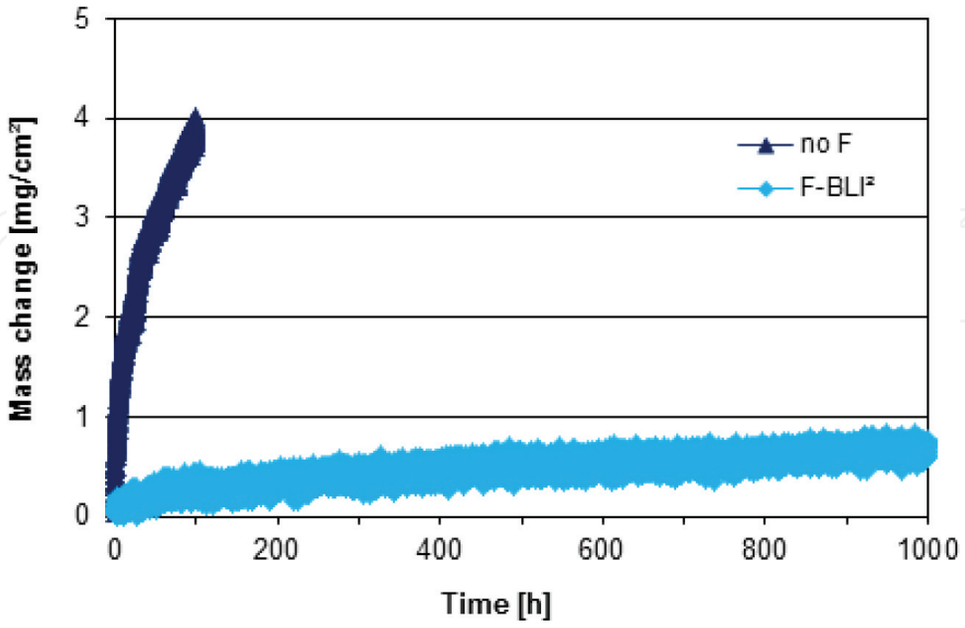


Figure 2. Thermogravimetric results of an untreated TiAl sample and a beamline fluorine-implanted TiAl sample during isothermal oxidation at 900°C in air.

effect. This positive result was achieved by applying the accurate amount of fluorine to the surface of the material [11]. In this case an optimized beamline implantation of fluorine was applied (F-BLI^2). This resulted in a rather low mass gain of less than 1 mg/cm^2 after 1000 h of oxidation at 900°C in air, while the final mass gain of the untreated specimen is almost four times higher, ca. 4 mg/cm^2, after a much shorter period of time (100 h).

The beneficial effect of fluorine on the oxide scale formation is shown in **Figure 3**. Only one side of the specimen was beamline implanted with fluorine prior to oxidation at 900°C in air, while the other side was not treated. It can be seen that the implanted side (**Figure 3a**) developed a thin oxide layer (1–2 μm) rich in alumina, while on the non-implanted side (**Figure 3b**), a thicker mixed scale (>20 μm) of Al_2O_3 + TiO_2 and nitrides was formed. The mixed scale consists of an outer layer of coarse rutile crystals, followed by a darker alumina-rich zone and a yellowish mixed oxide zone with nitrides. The Ni plating was applied prior to metallographic preparation to protect the oxide scales during preparation of the metallographic cross sections.

Alumina formation is promoted by optimized additions of the halogens fluorine, chlorine, bromine, and iodine to the surface of TiAl alloys. However, large amounts of halogens in the surface zone are very detrimental. They induce accelerated high-temperature corrosion [12, 13]. On the other hand, if the amounts of halogens are too low, there is no impact on the oxidation behavior of TiAl alloys, i.e., mixed scale formation.

This so-called halogen effect was first reported in [14–16]. Several models have been proposed in the literature to explain the positive effect of the halogens. One model is based on doping of titanium oxide by negatively charged halogen ions. By this negative charge, the rate of oxygen diffusion and hence TiO_2 growth is reduced [14]. A second model claims aluminum enrichment in the subsurface zone of the alloy due to formation of gaseous titanium halides and their evaporation which reduces the Ti content. This leads to an increased Al activity at the alloy/scale interface, which promotes the Al_2O_3 scale growth [15]. Contrarily, experimental results by Donchev et al. [17] have clearly shown that these two proposed models can be neglected to

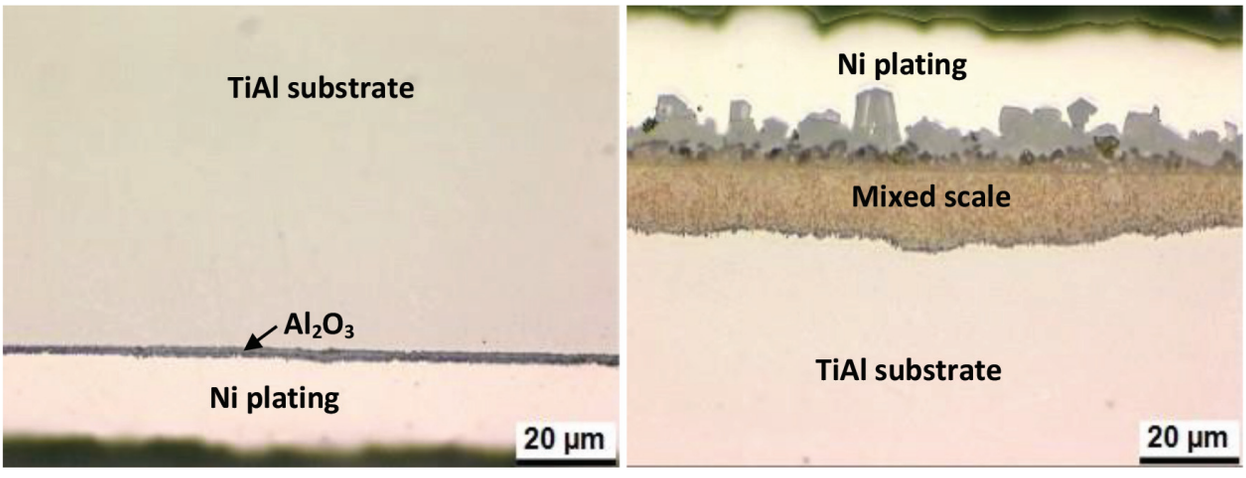


Figure 3. Cross-sectional LOM images showing the effect of beamline implantation of fluorine on one side (a) compared to the untreated side (b) after oxidation of a TiAl sample at 900°C for 100 h in air.

http://dx.doi.org/10.5772/intechopen.75696

describe the halogen effect. Their third model is based on the transport of aluminum via selective formation of gaseous Al halides. They diffuse outward from the substrate to the inner region of the naturally grown oxide scale where they are then oxidized to Al_2O_3 due to the steep increasing oxygen partial pressure. After an incubation period, the amount of Al_2O_3 formed in the inner region reaches a sufficient volume fraction to result in a pronounced reduction in the scale-growing kinetics [18]. In [17] the underlying thermodynamic mechanisms were mostly described for a chlorine beamline implantation. In a similar approach, the following data and equations are described for fluorine, which has shown to be more effective than chlorine during thermocyclic exposure [18]. Since AlF is the predominant carrier molecule for the aluminum transport, the reactions leading to Al_2O_3 formation can be signified as follows:

$$Al_{(s,TiAl)} + F \rightarrow AlF_{(g)} \Delta G_{900^\circ C} = -3.63 \times 10^5 \text{ J/mol} \tag{1}$$

$$4\ AlF_{(g)} + 3\ O_2 \rightarrow 2\ Al_2O_{3(s,oxide\ scale)} + 2\ F_2 \Delta\ G_{900^\circ C} = -1.19 \times 10^6 \text{ J/mol} \tag{2}$$

where Al is from the TiAl alloy and fluorine from different fluorine treatments (see below). Fluorine is released by Eq. (2) so that it can react again with Al from the substrate according to Eq. (1). The enthalpies of formation for both reactions are negative. Thus, they tend to react to the proposed products.

The minimum aluminum flux required via gaseous Al fluorides to sustain the growth of Al_2O_3 is determined by its growth kinetics, which follows the parabolic rate equation:

$$\Delta w = \left(k_p t\right)^{\frac{1}{2}} \tag{3}$$

where k_p is the parabolic rate constant ($g^2/cm^4 s$), Δw is the mass gain (g), and t is time (s). The flux of aluminum in the growing Al_2O_3 scale, J_{Al}^{ox}, is connected with the mass gain, i.e.,

$$J_{Al}^{ox} \propto \frac{d\Delta w}{dt} \tag{4}$$

and in the case of Al_2O_3 growth, it is found that

$$J_{Al}^{ox} = \frac{1}{48}\left(\frac{k_p}{t}\right)^{\frac{1}{2}} \qquad \frac{\text{mol Al}}{\text{cm}^2 \cdot \text{s}} \tag{5}$$

The k_p for Al_2O_3 scale growth at 900°C equals 5×10^{-13} g^2/cm^4 s [19]. Therefore, the flux J_{Al}^{ox} = 2×10^{-9} mol/cm^2 s after 60 s of oxidation. This value represents the minimum amount of aluminum which is necessary to maintain parabolic Al_2O_3 scale growth after this time. The flux, J_{Al}, of the gaseous Al fluorides within the nano−/micro-channels and cracks can be derived from the Hertz-Langmuir equation (kinetic theory of gases [20]). In the case of an aluminum mono-fluoride AlF, the equation is as follows

$$J_{AlF} = J_{Al} = 44.3 \frac{P_{AlF}}{\left(M_{AlF} T\right)^{\frac{1}{2}}} \qquad \frac{\text{mol Al}}{\text{cm}^2 \cdot \text{s}} \tag{6}$$

where P_{AlF} is the partial pressure of AlF in bar, M_{AlF} is the molecular weight of AlF (45.98 g/mol), and T is the absolute temperature (K). For AlF at 900°C (1173 K), Eq. 6 can be transformed to.

$$J_{Al} = 0.191 P_{AlF} \quad \frac{\text{mol Al}}{\text{cm}^2 \cdot \text{s}} \tag{7}$$

Therefore, by equalizing the two fluxes given by Eqs. (5) and (6), the minimum pressure P_{AlF}^{min} needed to sustain parabolic Al_2O_3 scale growth at 900°C and 60 s of oxidation can be calculated:

$$J_{Al}^{ox} = J_{Al} \tag{8}$$

$$2x10^{-9} = 0.191 P_{AlCl} \tag{9}$$

$$P_{AlF}^{min} = 1 \times 10^{-8}\ \text{bar} \tag{10}$$

There is a clear time and temperature dependency of P_{AlF}^{min}, decreasing with increasing time and/or decreasing temperature. The variation of P_{AlF}^{min} within the relevant calculated temperature range 700–1100°C for an oxidation time of 60 s is shown in **Table 1**. Obviously, the real partial pressure of the reacting halide has to be greater than the minimum predicted by the above-derived method. This has to be the case during the early stages of the oxidation process. Furthermore, it has to be taken into account that not all aluminum halide species will contribute to the positive effect.

According to thermodynamic equilibrium calculations, AlF is the most volatile species of the gaseous metallic fluorides within a certain F_2 pressure range. Consequently, Eqs. (1) and (2) are the principal reactions of concern from the standpoint of the beneficial fluorine effect. This also shows that at least two AlF molecules are required to react with each other to form Al_2O_3. Therefore, adsorption and nucleation on a surface are favored, because a direct reaction by gas collision is not likely.

With these assumptions kept in mind, thermodynamic calculations are useful to determine the minimum partial pressure of fluorine, $P_{F_2}^{min}$, necessary in reaction (1) to obtain P_{AlF}^{min}. The results from those calculations are presented in **Table 1**.

T/°C	$k_p(Al_2O_3)/g^2/cm^4s$	P_{AlF}^{min}/bar	$P_{F_2}^{min}$/bar
700	1×10^{-15}	4.3×10^{-10}	8.6×10^{-10}
800	5×10^{-14}	3.0×10^{-9}	6.0×10^{-9}
900	5×10^{-13}	1.0×10^{-8}	5.0×10^{-7}
1000	1×10^{-12}	1.6×10^{-8}	3.2×10^{-8}
1100	8×10^{-12}	4.5×10^{-8}	9.0×10^{-8}

The $k_p(Al_2O_3)$ values were obtained from the literature [19].

Table 1. Calculated minimum partial pressures of gaseous AlF and resulting pressures of F_2 which are necessary to sustain parabolic Al_2O_3 growth after 60 s of oxidation.

http://dx.doi.org/10.5772/intechopen.75696

As indicated by Eq. (1), it is required that fluorine is somehow present in the surface zone to react with the aluminum from the alloy to form gaseous Al fluorides. The implanted or "alloyed" fluorine has to develop a certain activity or partial pressure. Since the thermodynamic data for the fluorine activity in solid solution is not available, data for the F_2 partial pressure which can be calculated are taken into account for the following discussion. The partial pressure of elemental fluorine, P_{F2}, can be derived from the following equation:

$$P_{F_2} = a_F^2 \exp\left(\frac{-\Delta G}{RT}\right) \tag{11}$$

where ΔG is the Gibbs free enthalpy for the formation of F_2 and a_F is the chemical activity of F in the TiAl substrate. Unfortunately, no data exist for both of these parameters. In addition it has to be kept in mind that the system is not closed. During high-temperature exposure, fluorine can be released by outward diffusion of gaseous species without reacting with Al before a closed alumina scale can block this [18]. Hence, the P_{F2} at the alloy/scale interface can only be approximated to be within a certain range. However, it will be shown that meaningful results can be obtained by making such an approximation.

Also, an upper limiting P_{F2} value for the beneficial fluorine effect ($P_{F_2}^{max}$) has to be approximated. This approximation is based on the competition of Al and Ti oxide formation. As discussed earlier, the formation and subsequent growth of the Al_2O_3-rich scale requires the adsorption of the aluminum fluoride species onto the surfaces of pores and micro-cracks within the oxide. The extent of aluminum adsorption would be expected to increase with an increase in the summed partial pressure of the reactive Al fluoride species, $\sum P_{AlFx}$, up to the point where the rate of aluminum supply is sufficient to sustain parabolic Al_2O_3 growth kinetics, i.e., when $\sum P_{AlFx} = P_{\Sigma AlF_x}{}^{min}$. Beyond this point the rate of Al_2O_3 growth would be solid-state diffusion controlled and therefore independent of P_{AlFx}. The extent of titanium adsorption and subsequent TiO_2 growth would be equally expected to increase with increasing partial pressure of the volatile Ti halide species, $\sum P_{TiXy}$. However, the rate of TiO_2 growth is significantly greater than that of Al_2O_3 [21]. Therefore, if it is assumed that the probability for oxidation is the same for all chemisorbed species and that non-protective inner-scale formation occurs when the rate of TiO_2 growth exceeds that of Al_2O_3; then, it can be approximated that the beneficial fluorine effect can only occur if $\sum P_{TiFy} < \sum P_{\Sigma AlF_x}{}^{min}$ (stoichiometry and molar volume of the oxides are being neglected in this approximation since no significant changes in the results would occur). As will be shown in the following, this essentially equates to $P_{F_2}^{max}$ being set by $P_{TiF3} = P_{AlF}^{min}$. When $P_{F_2} > P_{F_2}^{max}$, the predominance of aluminum oxidation is not possible, and the formation of a non-protective TiO_2-Al_2O_3 or TiO_2-rich scale occurs instead.

$P_{F_2}^{min}$ and $P_{F_2}^{max}$ can be obtained from thermodynamic calculations. The main aim of the thermodynamic calculations is to quantify the P_{X2} "corridor" (and by this the level of the necessary halogen reservoir) in which the beneficial halogen effect can operate. The potential reactions considered in these calculations are given in the following for fluorine. The calculations were conducted using the thermodynamic software packages ChemSage and FactSage [22].

Apart from the formation and oxidation of $AlF_{(g)}$ given by reactions (1) and (2), the following reactions must also be considered because their enthalpy is negative:

$$Al_{(TiAl)} + F_2 \rightarrow AlF_{2(g)}; \Delta G = -6.64 \times 10^5 \quad (12)$$

$$Al_{(TiAl)} + 1.5\ F_2 \rightarrow AlF_{3(g)}; \Delta G = -1.14 \times 10^6 \quad (13)$$

$$Ti_{(TiAl)} + 0.5\ F_2 \rightarrow TiF_{(g)}; \Delta G = -1.92 \times 10^5 \quad (14)$$

$$Ti_{(TiAl)} + F_2 \rightarrow TiF_{2(g)}; \Delta G = -6.57 \times 10^5 \quad (15)$$

$$Ti_{(TiAl)} + 1.5\ F_2 \rightarrow TiF_{3(g)}; \Delta G = -1.11 \times 10^6 \quad (16)$$

$$Ti_{(TiAl)} + 2\ F_2 \rightarrow TiF_{4(g)}; \Delta G = -1.41 \times 10^6 \quad (17)$$

$$2\ TiF_{(g)} + 2\ O_2 \rightarrow 2\ TiO_{2(s)} + F_2; \Delta G = -1.09 \times 10^6 \quad (18)$$

$$TiF_{2(g)} + O_2 \rightarrow TiO_{2(s)} + F_2; \Delta G = -7.93 \times 10^4 \quad (19)$$

Unlike other halogens [19], the enthalpies of the oxidation of the fluorides with a high oxygen state of the cation are positive for both metals Al and Ti:

$$4\ AlF_{3(g)} + 3\ O_2 \rightarrow 2\ Al_2O_{3(s)} + 6\ F_2; \Delta G = +1.94 \times 10^6 \quad (20)$$

$$4\ AlF_{2(g)} + 3\ O_2 \rightarrow 2\ Al_2O_{3(s)} + 4\ F_2; \Delta G = +3.66 \times 10^4 \quad (21)$$

$$TiF_{3(g)} + O_2 \rightarrow TiO_{2(s)} + 1.5\ F_2; \Delta G = +3.76 \times 10^5 \quad (22)$$

$$TiF_{4(g)} + O_2 \rightarrow TiO_{2(s)} + 2\ F_2; \Delta G = +6.79 \times 10^5 \quad (23)$$

From the enthalpies of the reactions (10), (18), and (19), it can be concluded that only AlF leads to the fluorine effect, i.e., there is no thermodynamic driving force for the oxidation of the stable molecules AlF_2 or AlF_3. As a consequence of this, all the thermodynamic calculations for $P^{min}_{Al_xF_y}$ and $P^{max}_{Al_xF_y}$ are based on the assumption that Al_2O_3 growth is sustained only via AlF transport. The maximum pressure $P^{max}_{F_2}$ is reached if the titanium fluorides start to get relevant, i.e., $P_{Ti_xF_y}$ equals P^{min}_{AlF} . In **Figure 4** the pressures of the gaseous fluorides at 900°C are presented. It can be clearly seen that $AlF_{(g)}$ is the predominant species.

In the envisaged temperature range above 700°C where oxidation protection of TiAl components is needed, a positive fluorine effect is established (**Figure 5**). The corridor for the so-called fluorine effect widens with increasing temperature and spans several orders of magnitude of the fluorine pressure. The values for $P^{min}_{F_2}$ rise steadily with increasing temperature, while for $P^{max}_{F_2}$ a type of plateau is reached at about 1000°C. The values of $P^{max}_{F_2}$ at 900 and 1100°C are slightly lower than the one at 1000°C. The limits for the other halogens are similar (see Appendix **Figures A1**, **A2**, **A3**).

http://dx.doi.org/10.5772/intechopen.75696

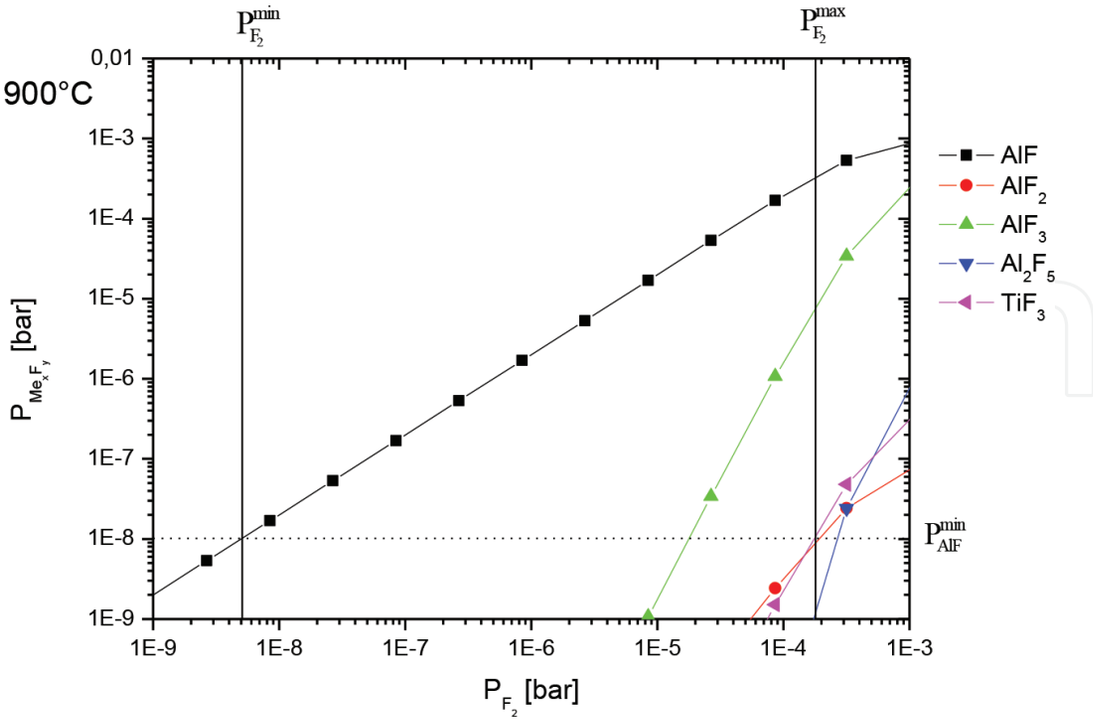


Figure 4. Calculated partial pressures of the gaseous metal fluorides versus elemental fluorine partial pressure at 900°C.

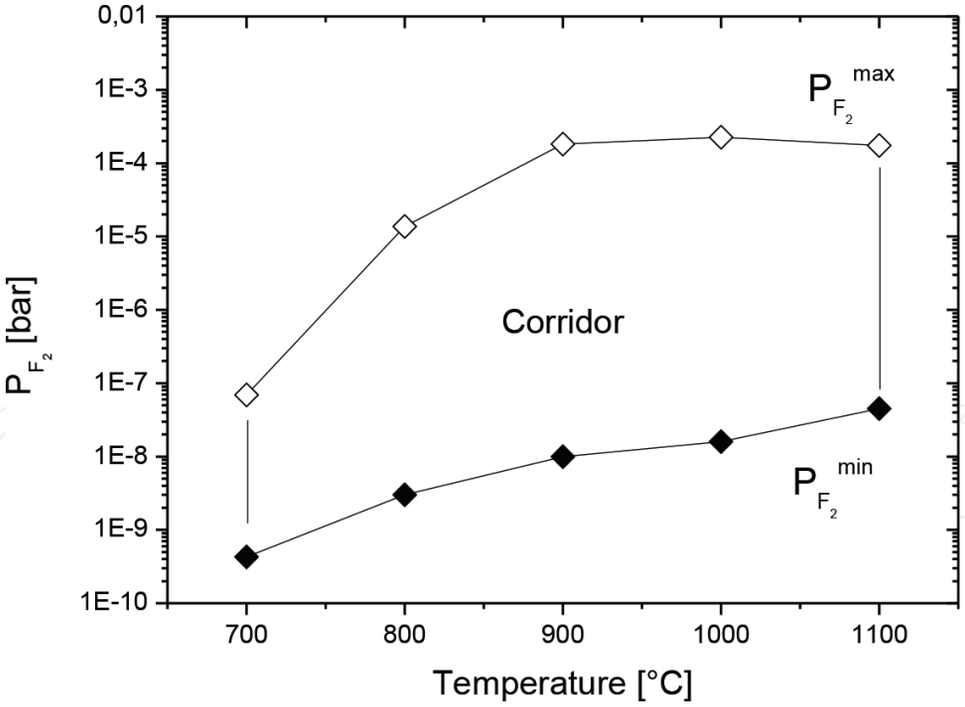


Figure 5. P_{F2} limits of the fluorine effect.

Furthermore, evaporation of stable titanium fluorides during heating up has to be considered (s. **Table 2**) because the higher-valence titanium fluorides are very stable and do not show much tendency to form titanium oxide (see reactions (20) and (21)). This leads to a fluorine loss

Temperature/°C	$p(TiF_{4(g)})$/bar
100	5.10×10^{-5}
200	3.08×10^{-3}
300	1.70×10^{-0}
400	8.40×10^{-0}
500	6.36×10^{-6}
600	1.20×10^{-10}

Table 2. Calculated partial pressures of $TiF_{4(g)}$ during heating up.

which has to be overcome by an "over-doping." On the other hand, this can have a certain buffering effect if too much fluorine is applied locally.

The calculations and consideration confirm the positive fluorine effect if the oxidation temperature is sufficiently high, the heating-up period is kept short, and if an overdose of fluorine (but not so high to induce corrosion) is applied in order to account for fluorine losses during heating to oxidation temperature.

3. Fluorination

The positive results of the optimized F-BLI^2 shown in **Figure 1** were achieved during isothermal exposure at 900°C in air. For the technical use of TiAl components, protection under thermocyclic conditions for much longer exposure times is an obligatory requirement. Additionally, different fluorination techniques had to be developed because beamline implantation can only be used for laboratory-scale samples with flat surfaces and not for technical components with complex structures, e.g., turbo charger rotors. Therefore, several attempts have been undertaken to apply a fluorine treatment which is independent of any sample geometry. First, a liquid-phase treatment by dipping in aqueous $HF_{(aq.)}$ was utilized [23]. The concentration of the acid, the temperature, and the dipping time had to be adjusted. The concentration is very relevant because the etching of the metallic surface must be limited. After optimization the best results were achieved by the following set of parameters, dipping in 0.1 mol% $HF_{(aq)}$ for 2 h at room temperature (RT) which can be seen in **Figure 6**.

A second liquid-phase treatment was performed by spraying halogen-containing polymers uniformly over the whole surface of different TiAl samples at RT and simple drying in air afterward. Depending on the polymer and it's amount used, a mass loss is observed after the beginning of oxidation which levels off to alumina kinetics during further exposure (**Figure 7**). This mass loss is caused by the decomposition of the polymer and evaporation of the organic residues. The released fluorine reacts with the metal surface, thus activating the fluorine effect. Samples of the technical second-generation alloy γ-MET (Ti-46.5Al-4(Cr, Nb, Ta, B)) were exposed thermocyclically at 900°C in air. The samples were placed in the hot furnace, kept at temperature for 24 h, removed from the hot furnace, cooled to RT within about 15 min,

http://dx.doi.org/10.5772/intechopen.75696

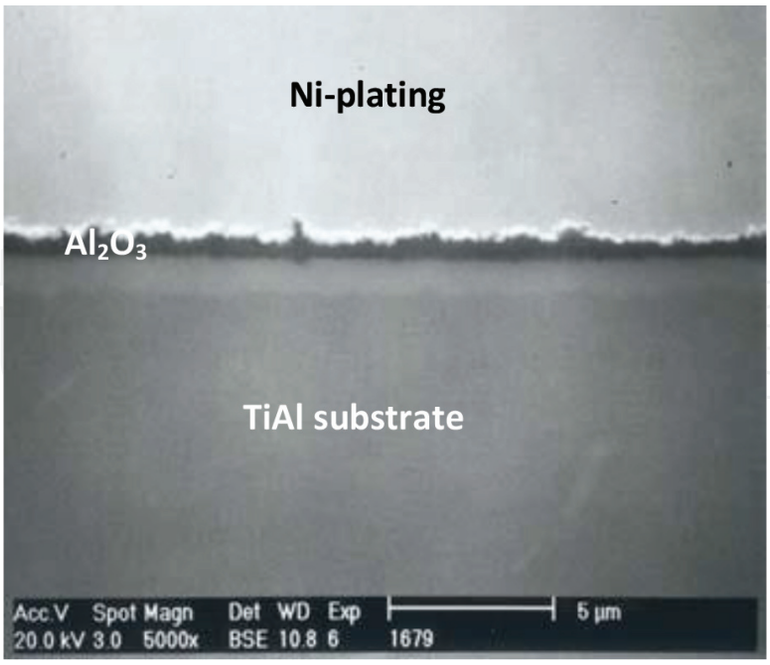


Figure 6. SEM/BSE image of a TiAl specimen treated with 0.1 mol% HF for 2 h at RT and oxidized for 100 h at 900°C in air.

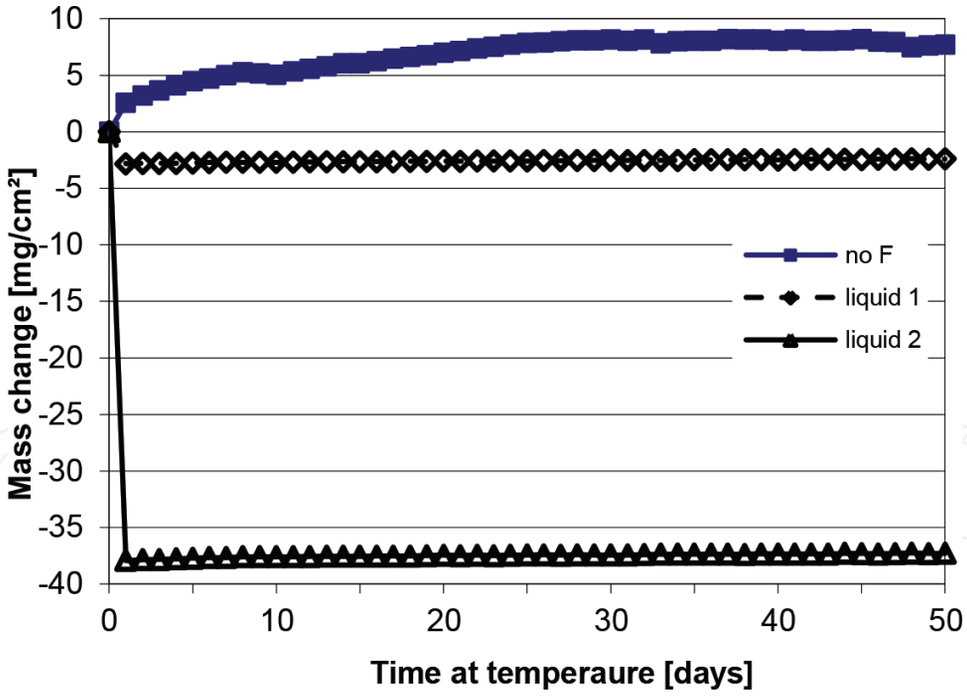


Figure 7. Mass change data of three TiAl specimens exposed thermocyclically at 900°C in air. One sample is untreated, and the two other samples are liquid-phase F-treated.

weighed, and put back into the hot furnace after 1 hour, thus resulting a 25 h cycle test. The untreated sample reveals a mass gain which is interrupted several times by minor mass losses due to spallation of parts of the oxide scale. Spallation can occur if the stresses caused by the

CTE mismatch between ceramic oxide and metallic substrate exceed a certain level. The final mass gain after 50 days of exposure (= 1200 h) is about 8 mg/cm^2. The mass change behavior of the two treated specimens is characterized by a mass loss during the first day of exposure due to evaporation of the organic residues of the polymer. Depending on the polymer, this mass loss can vary between 1 and almost 40 mg/cm^2. After this mass loss, a very slow-growing scale and absolutely no spallation of any parts of the scale were observed. The mass gain during the 49 remaining days of exposure was less than 2 mg/cm^2 for both F-polymer-treated samples.

Besides the described liquid-phase treatments, fluorination via the gas-phase directly at elevated temperatures has also been proven to be successful. The first attempt has been made by the decomposition of solid fluorine-containing polymers. TiAl samples were placed in a hot furnace together with small amounts of a solid fluorine-containing polymer. During the initial hours of exposure, the polymer decomposes and fluorine is released. The fluorine reacts with the specimen to allow the fluorine effect to operate. The whole process is performed under laboratory air. No protective gas is needed. In **Figure 8** results of the same thermocyclic 25 h cycle test are presented. The F-treated sample showed a pronounced mass gain during the first day due to uptake of fluorine and oxygen, but during the second day, the mass gain rate has dropped, and the total mass gain during the next 49 days of exposure stayed below 1 mg/cm^2.

Beamline ion implantation (BLI^2) cannot provide total protection for technical TiAl compounds. Therefore, a different implantation technique has to be used. The plasma immersion ion implantation (PI^3) allows implantation of specimens with more complex geometries [24]. During this treatment the samples are placed in a vacuum chamber and a negative charge is applied. The fluorine-containing gas is led into the chamber and the plasma is ignited. Due to the high voltage, the fluorine cations are accelerated to the surface of the specimen so that this is implanted

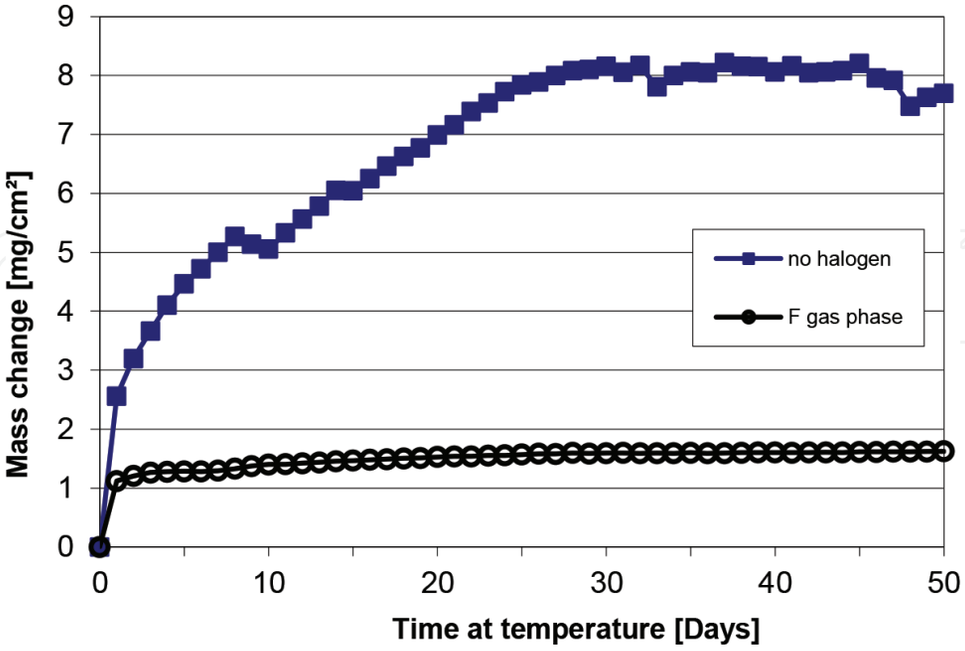


Figure 8. Mass change data of two TiAl specimens exposed thermocyclically at 900°C in air. One sample is untreated and the second is gas-phase F-treated.

http://dx.doi.org/10.5772/intechopen.75696

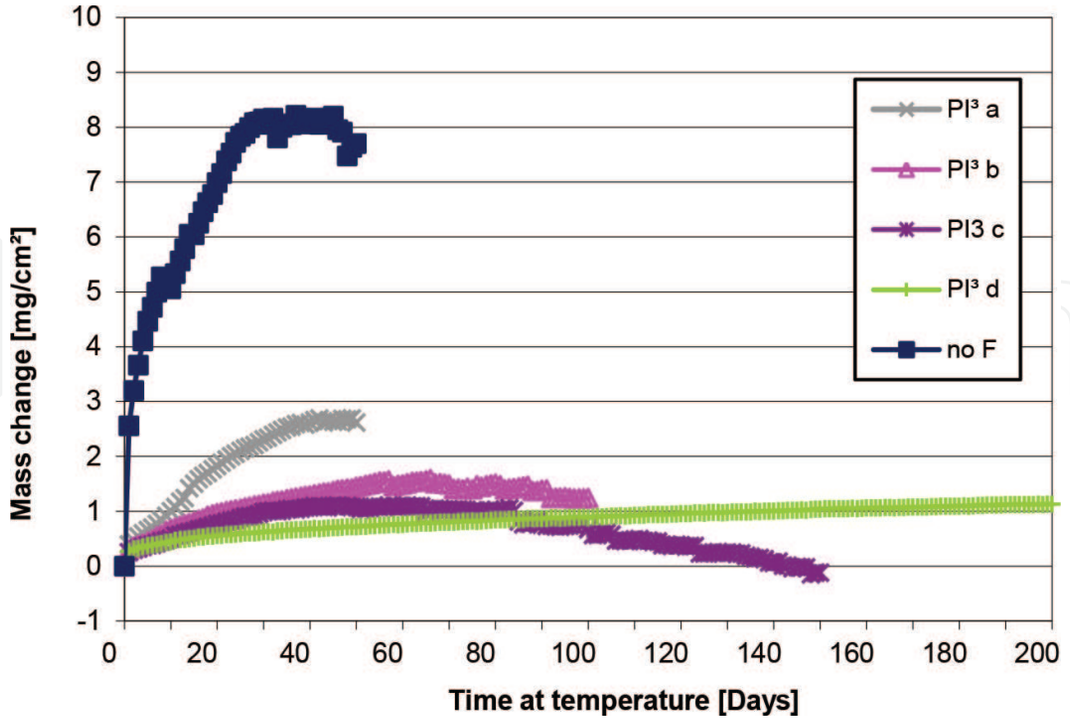


Figure 9. Mass change data of an untreated and four F-PI^3-treated TiAl specimens exposed thermocyclically at 900°C in air.

completely. Elemental F_2 gas or other fluorine-containing gases such as CH_2F_2 can be used. After optimization of this technique, thermocyclic long-term oxidation protection of TiAl samples for 4800 h at 900°C in air was achieved (**Figure 9**). Only the sample named PI^3-d showed slow-growing alumina kinetics over the whole period of exposure (200 days = 4800 h), while the three other F-PI^3 implanted specimens revealed at better behavior than the untreated sample, but further optimization was needed. Their mass gains are higher than the one of the sample PI^3-d, and some mass losses due to partial spallation of the oxide scale can be seen even leading to a final negative mass change value of the sample PI^3-c after 150 days of exposure. It can be said that the process was finally optimized to result in stable oxidation protection of TiAl specimens.

An evaluation of the mass changes of several samples after each day during thermocyclic exposure can be seen in **Figure 10**. The differences of the masses of the specimens treated with fluorine by different techniques are almost zero from day 2 of exposure to the end, while the untreated sample reveals a much larger scatter. During the first days of exposure, the difference gets smaller. The observable mass losses were caused by spallation. The higher mass gains directly afterward were due to formation of a new mixed oxide scale at the spalled areas. Even during the last days of exposure, the variation of the mass of the untreated sample is always higher than the ones of the F-treated specimens.

3.1. Long-term protection

The 24 h cycle test was prolonged for 1 year, i.e., 365 days (= 8760 h), to investigate the long-term stability of the fluorine effect. In **Figure 11** the mass change data of the exposed samples

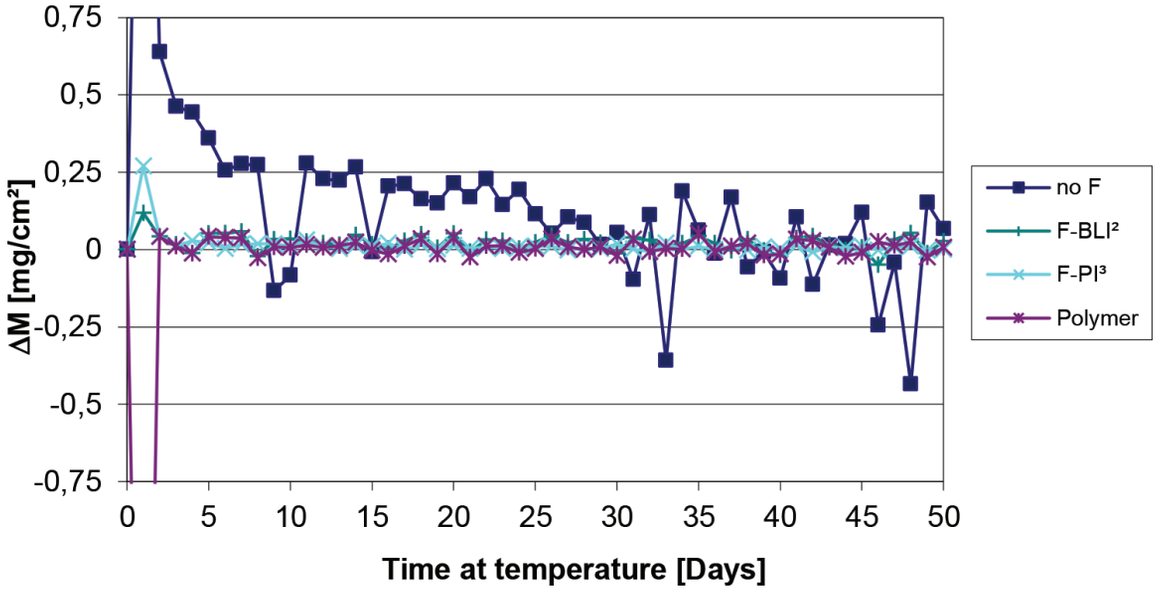


Figure 10. Mass change between each day of an untreated and three different F-treated TiAl specimens exposed thermocyclically at 900°C in air for 50 days.

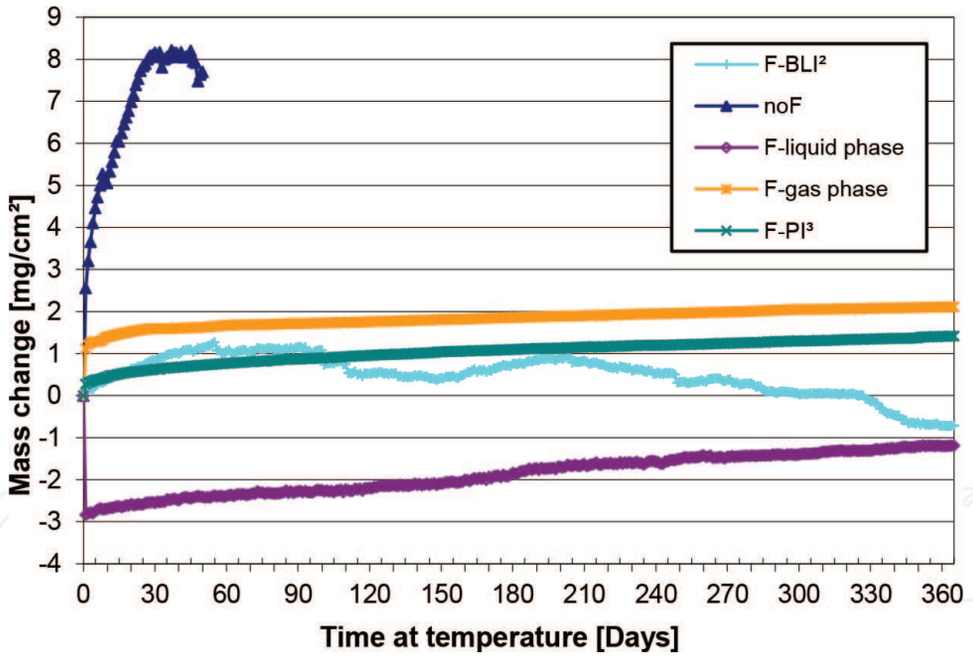


Figure 11. Mass change data of an untreated and four different F-treated specimens exposed thermocyclically at 900°C in air.

are depicted. The F-BLI^2 implanted sample had a negative mass change at the end of the test. This was caused by spallation of parts of the oxide at areas of the specimen where a mixed scale has formed. This sample was not protected at the edges due the limitation of the BLI^2 process so that ordinary mixed scale formation took place at these spots. During the fast cooling to RT, parts of this mixed scale spalled off. The other three F-treated specimens did

http://dx.doi.org/10.5772/intechopen.75696

not show any tendency to spallation. The mass gain was slow and steady. The reasons for the mass loss of the sprayed specimen and the mass gain of the gas-phase-treated specimen after the first day are described above. The PI^3 also provides total coverage. The F-treated samples do not show any weakness in the protective fluorine effect. This effect is expected to the last much longer. Post-experimental investigations illustrate the nature of the scales formed during exposure. The appearance of the specimens reflects their mass change data. The untreated sample is covered with a yellowish scale which has partly spalled (**Figure 12a**). The edges of the F-BLI^2 sample are covered with a yellow/brown mixed scale, while the faces are gray, which indicates the protective alumina layer (**Figure 12b**). The faces were implanted, but the edges could not be treated due to the limits of the beam process. The PI^3 process on the other hand is also capable of implanting the edges; hence, the sample appears totally gray (**Figure 12c**). The sprayed sample looks white (**Figure 12d**). This is caused by the residues of the spray which were oxidized above the protective alumina layer. This will be subsequently shown in detail in the metallographic cross sections.

The metallographic cross sections reveal the nature of the oxide scales. The light optical microscope (LOM) images show the differences of the scales formed during oxidation on the surfaces of the exposed samples. The mixed scale on the untreated sample after 50 days of exposure is roughly 100 μm thick and exhibits a lot of cracks (**Figure 13a**). The mixed scale consists of an outer rutile layer, followed by an alumina layer and a mixed oxide nitride scale

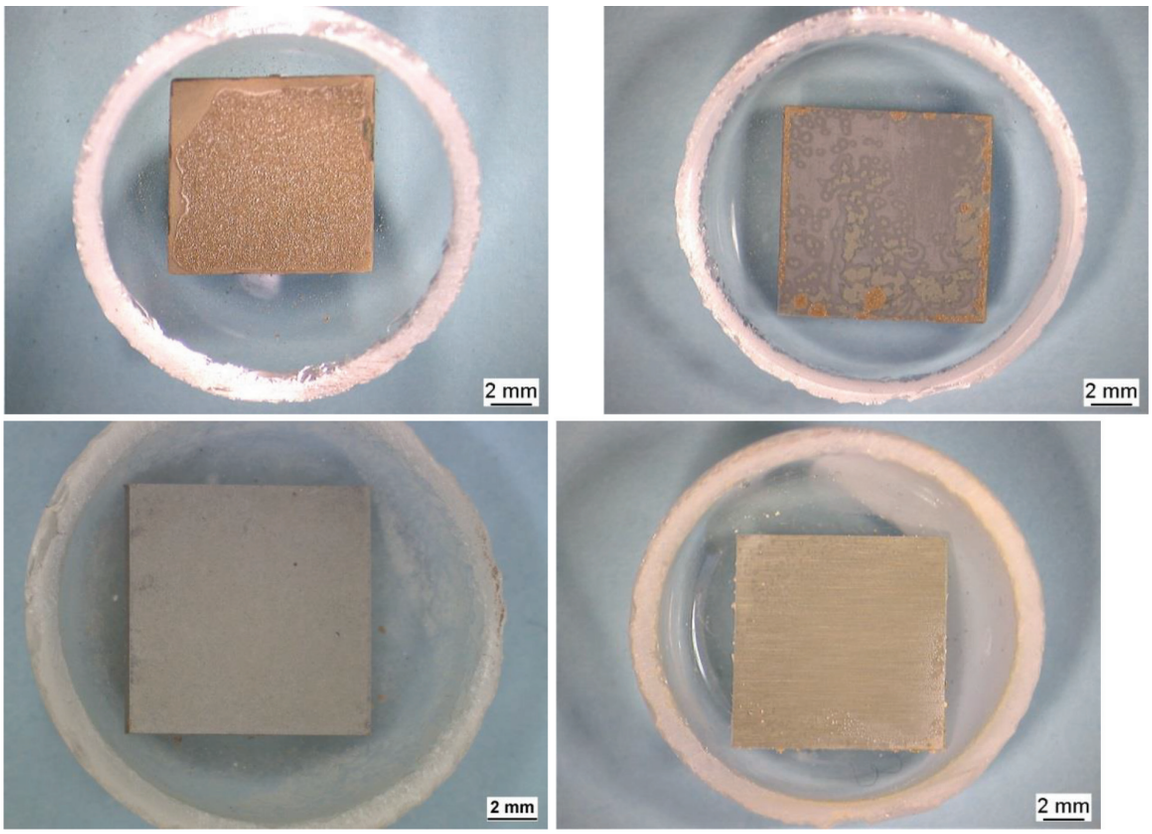


Figure 12. Optical appearance of the exposed TiAl samples after thermocyclic oxidation at 900°C in air: (a) untreated sample after 50 days, (b) F-BLI^2, (c) F-PI^3, and (d) F-sprayed all three after 365 days.

above the substrate. The LOM images of the treated specimens indicate the thin layers where the fluorine effect had functioned (**Figure 13b–d**).Accelerated oxidation occurred at the unimplanted edges of the F-BLI^2 sample (**Figure 14a**, **b**). The metallic cross section is reduced due to spallation and renewed oxidation (**Figure 14 a**). The transition of the thick mixed scale to the areas with the thin alumina layer can be seen. Here, the fluorine effect via the BLI^2 is still working. The mixed scale is undulated and roughly 50–100 μm thick (**Figure 14b**).

Scanning electron microscopic investigations coupled with energy dispersive X-ray spectroscopy (SEM/EDX) provide a better grasp of the microstructure and composition of the scales. The images of the F-treated specimens look similar; hence, only one sample is presented here. The F-spayed sample is covered with a thin protective alumina layer on all faces (**Figure 15a**). This layer is approximately 2–3 μm thick (**Figure 15b**). Underneath this layer some fluorine was detected locally in some spots at the metal/oxide interface (**Figure 16a**). This was proven by EDX (**Figure 16b**). The scale is very thin (1–2 μm), thus Ni from the Ni plating and Ti, Cr, and Nb from the substrate were detected next to Al, O, and F from the scale.

Electron probe microanalysis (EPMA) provides the elemental distributions within the scales. Fluorine was found at two spots underneath the thin alumina layer (**Figure 17a**). The oxide layer consists predominantly of Al and O (**Figure 17b**, **c**) with some titanium oxide on the outer surface (**Figure 17d**), which was formed during the incubation period. The metallic subsurface

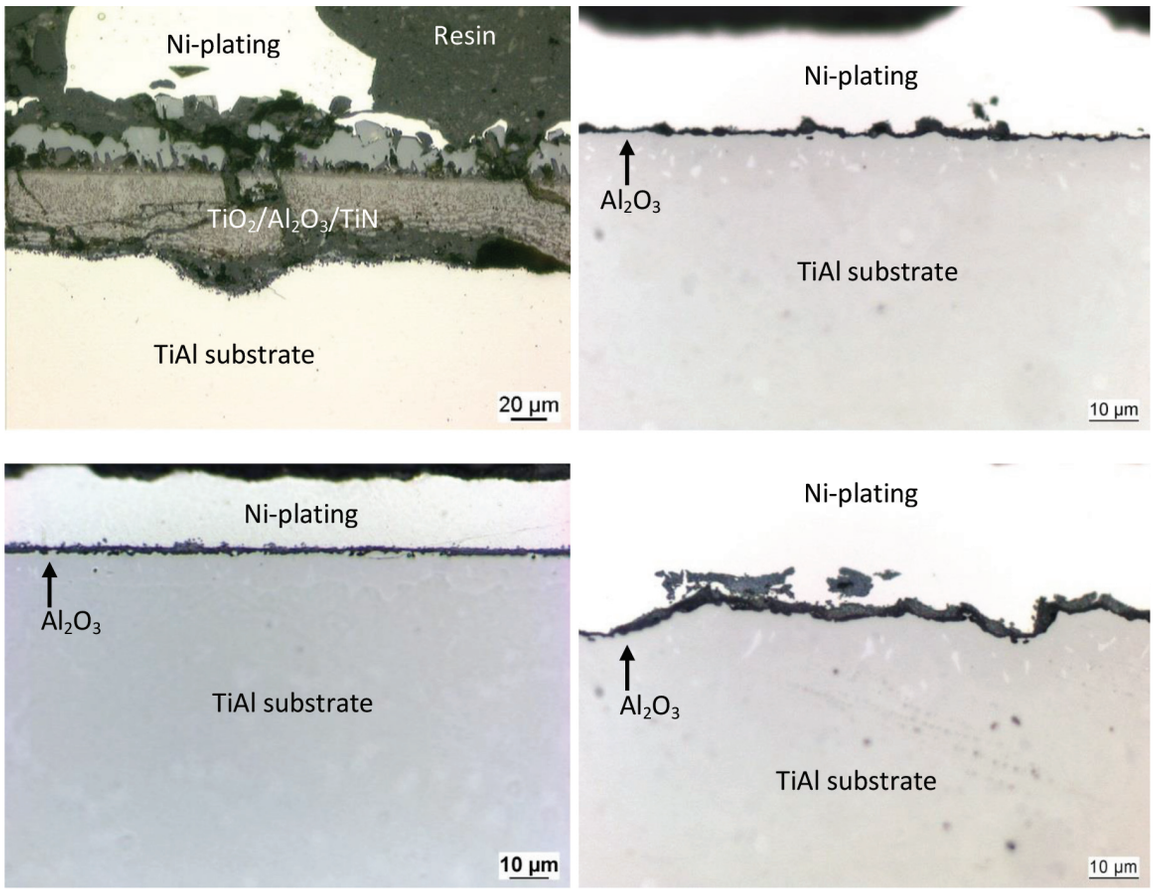


Figure 13. LOM images of the exposed TiAl samples after thermocyclic oxidation at 900°C in air: (a) untreated sample after 50 days, (b) F-BLI^2, (c) F-PI^3, and (d) F-sprayed all three after 365 days.

http://dx.doi.org/10.5772/intechopen.75696

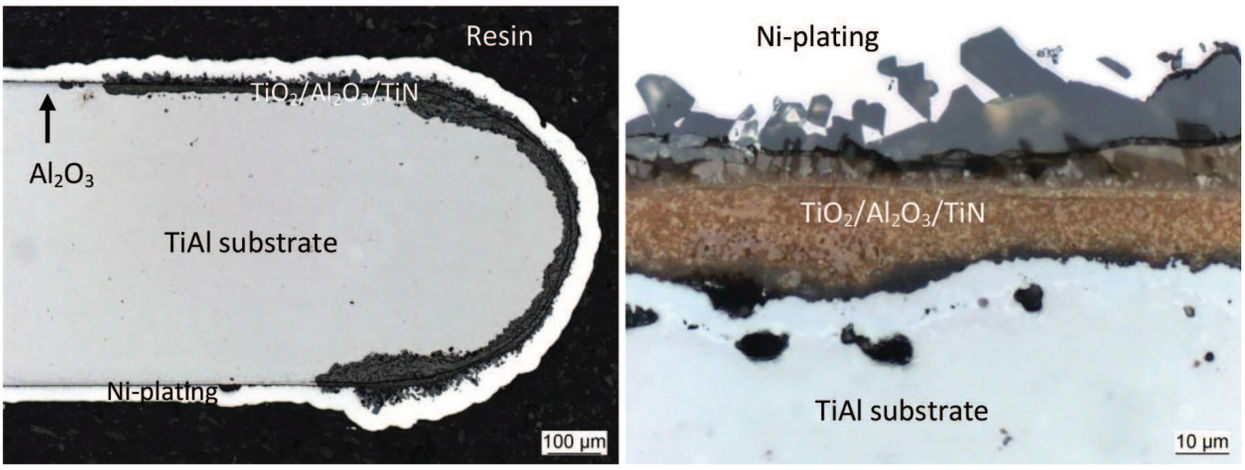


Figure 14. LOM images of the exposed F-BLI^2 sample after thermocyclic oxidation at 900°C for 365 days in air: (a) overview and (b) detailed image of the mixed scale.

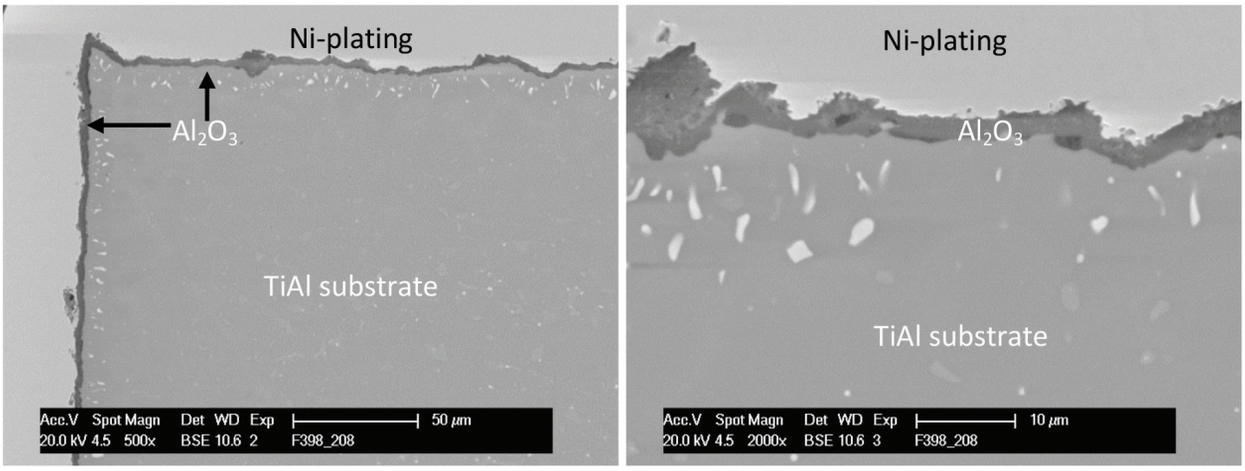


Figure 15. SEM images of the F-sprayed sample after thermocyclic oxidation at 900°C for 365 days in air: (a) overview of an edge and (b) detailed image of the thin alumina layer.

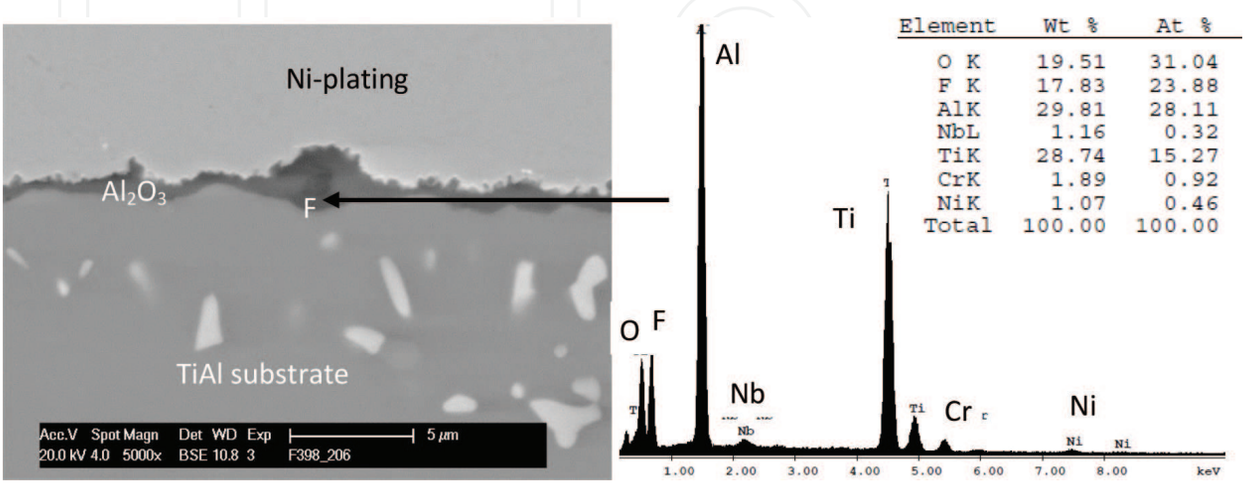


Figure 16. SEM/BSE image (a) and EDX spectrum (b) of the F-BLI^2 sample after thermocyclic oxidation at 900°C for 365 days in air.

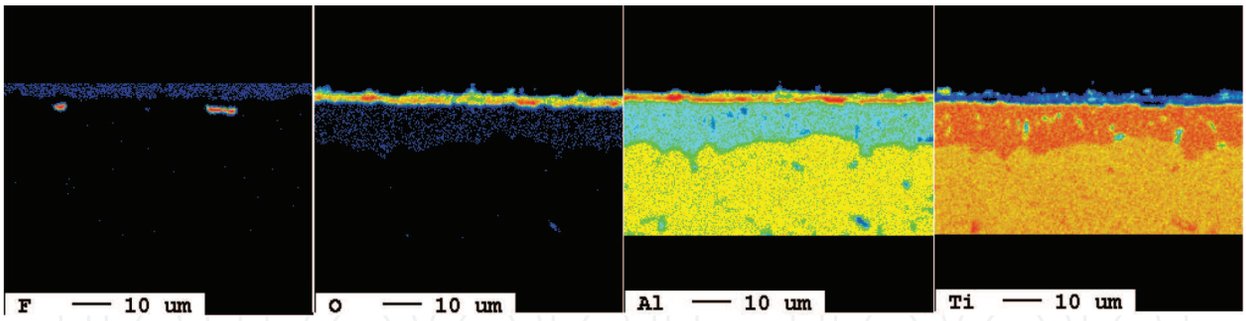


Figure 17. EPMA elemental distribution images of F (a), O (b), Al (c), and Ti (d) of the F-PI[3] sample after thermocyclic oxidation at 900°C for 365 days in air.

zone is depleted in Al due to alumina formation via the fluorine effect. This can be seen in the elemental distributions (**Figure 17c,d**), while it is hard to see this feature in the corresponding SEM/BSE image (**Figure 18**). The additional elements such as Nb or Cr are enriched in precipitates also in the subsurface zone. Those can be correlated to the bright spots in **Figure 18**. The fluorine spots underneath the alumina layer can be seen in this figure, too.

3.2. TiAl components

Turbocharger rotors as examples for technical TiAl components have been tested as well. The components were used in the as-received state. Fluorination was performed by spraying. The samples were exposed at 1050°C for up to 1200 h in laboratory air. In every 100 h the samples were taken out of the hot furnace cooled to RT outside the furnace, images were made, and

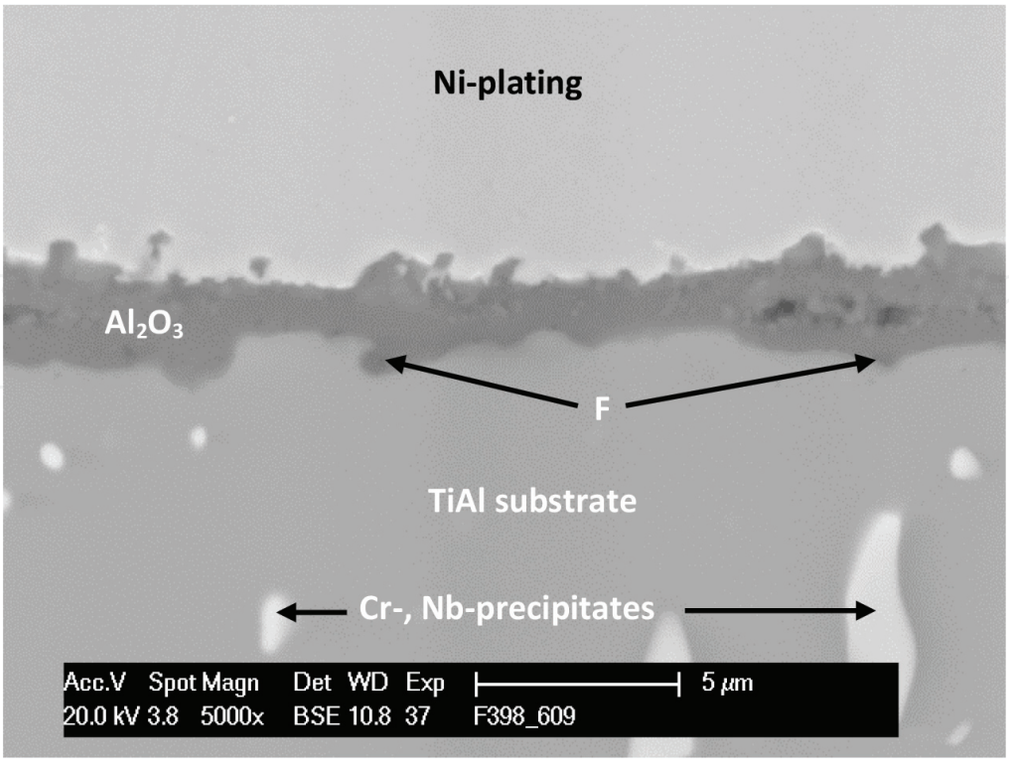


Figure 18. Corresponding SEM/BSE image of the F-PI[3] sample after thermocyclic oxidation at 900°C for 365 days in air.

http://dx.doi.org/10.5772/intechopen.75696



Figure 19. Macroscopic images of an untreated turbocharger rotor before (a), after 100 h (b), and 1200 h (c) of oxidation at 1050°C in laboratory air.

after 1 hour, the samples were put back in the hot furnace. The untreated specimens show severe spallation of the oxide scale (**Figures 19**, **20b–c**). This happened during each cooling down very shortly after removing from the furnace, while the sample was still hot. The load-bearing cross section of the blades is reduced due to this attack. Exposure at 1050°C can even lead to the total destruction of the component only by oxidation itself if the material is more sensitive to oxidation, i.e., due to changes in the chemical composition (**Figure 20a–c**). In contrast the fluorine treatment protected the rotors for the whole period of exposure. The treated samples only change color. The shown sample appears yellowish after 100 h and only became a bit darker (**Figure 21a–c**). No sign of any spallation is visible.



Figure 20. Macroscopic images of the second untreated TiAl rotor with a different chemical composition before (a), after 100 h (b), and totally destroyed after 1200 h (c) of oxidation at 1050°C in laboratory air.



Figure 21. Macroscopic images of an F-treated turbocharger rotor after spraying (a), after 100 h (b), and 1200 h (c) of oxidation at 1050°C in laboratory air.

4. Conclusions

The results show the remarkable effect of several optimized fluorine treatments by improving the oxidation resistance of TiAl alloys. The oxidation mechanism of the TiAl alloys is changed from non-protective mixed scale formation to alumina formation via the halogen effect if a defined amount of halogen is applied at the surface. Fluorine is the best doping element. Its effect lasts as long as 1 year under thermocyclic conditions without any signs of weakness, e.g., spallation. If only oxidation is taken into account, the temperature capability of TiAl alloys can be raised up to at least 1050°C. The fluorine content has to reach a certain minimum level to obtain the effect to operate, but an upper level must not be exceeded. Otherwise, negative fluorine corrosion occurs which would lead to accelerated oxidation. After optimized fluorine treatment, i.e., PI^3; liquid-phase treatment, e.g., by spraying; or a gas-phase treatment, total coverage of the surface can be achieved. With such a treatment, the use of TiAl components at elevated temperatures could be possible with all the advantages of this lightweight material regarding the efficiency of, e.g., jet engines or automotive engines.

Acknowledgements

The work was funded by the German Federal Ministry for Economic Affairs and Energy via the German Federation of Industrial Research Associations which is gratefully acknowledged by the authors. The fruitful discussions with Prof. B. Gleeson and Prof. M. Schütze concerning the mechanism of the halogen effect are also acknowledged.

A. Appendix

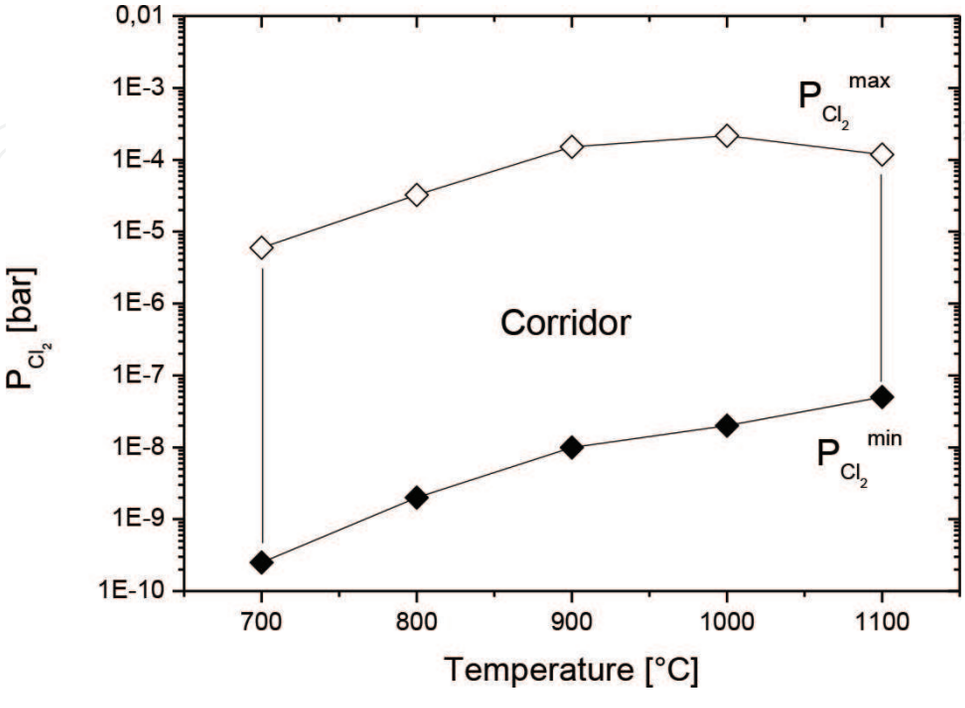


Figure A1. P_{Cl2} limits for the chlorine effect.

http://dx.doi.org/10.5772/intechopen.75696

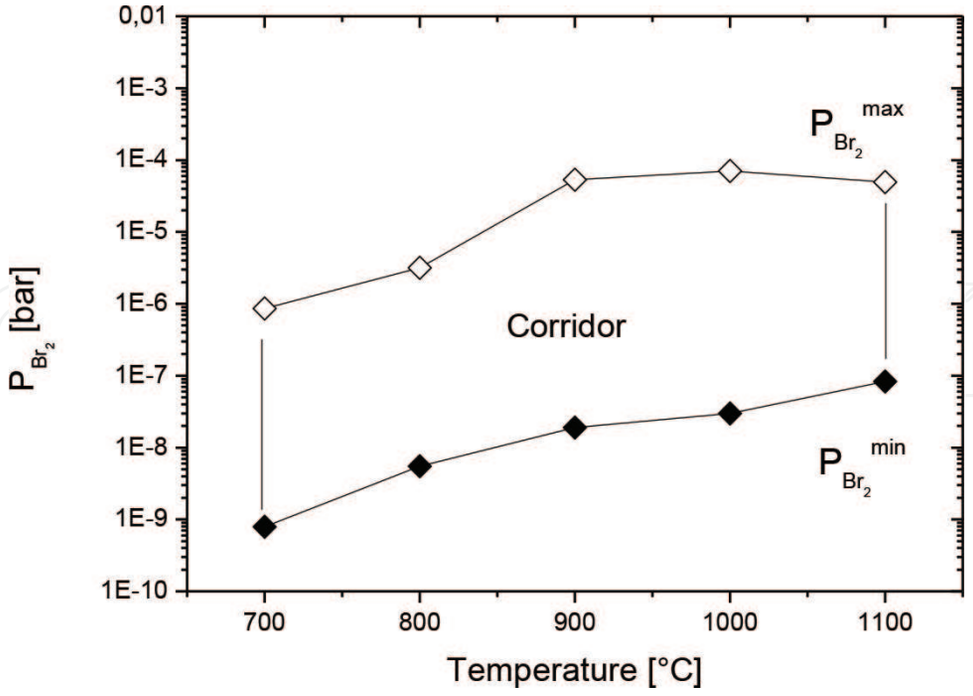


Figure A2. P_{Br2} limits for the bromine effect.

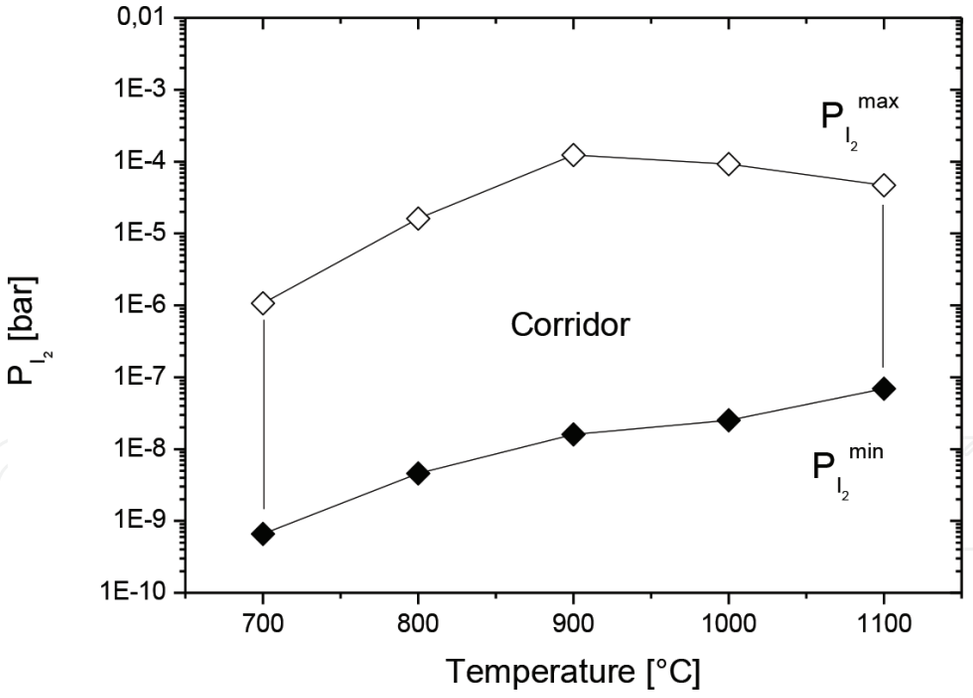


Figure A3. P_{I2} limits for the iodine effect.

Author details

Alexander Georg Donchev and Mathias Christian Galetz*

*Address all correspondence to: galetz@dechema.de

DECHEMA-Forschungsinstitut, Frankfurt am Main, Germany

References

[1] Clemens H, Mayer S. Advanced Engineering Materials. 2013;**15**:191

[2] Schwaighofer E, Clemens H, Mayer S, Lindemann J, Klose J, Smarsly W, Güther V. Intermetallics. 2014;**44**:128

[3] Appel F, Oehring M, Paul J. Gamma Titanium Aluminide Alloys. Weinheim, Germany: WILEY-VCH; 2011

[4] Appel F, Oehringe M. In: Leyens C, Peters M, editors. Titanium and Titanium Alloys. Weinheim, Germany: WILEY-VCH; 2003. p. 89

[5] Leyens C. In: Leyens C, Peters M, editors. Titanium and Titanium Alloys. Weinheim, Germany: WILEY-VCH; 2003. p. 187

[6] Shida Y, Anada H. Corros. Science. 1993;**35**:945

[7] Luthra KL. Oxidation of Metals. 1991;**36**:475

[8] Dettenwanger F, Schumann E, Rakowski J, Meier GH, Rühle M. Material Science Forum. 1997;**211**:251-254

[9] Schütze M. In: Holmes DR, editor. Protective Oxide Scales and their Breakdown. Chichester, UK: WILEY-Chichester; 1997

[10] Donchev A, Schütze M, Kolitsch A, Yankov R. Material Science Forum. 2012;**1061**:706-709

[11] Donchev A, Zschau H-E. M. Schütze. In: Brillas E, Cabot P-L, editors. Trends in Electrochemistry and Corrosion at the Beginning of the 21st Century. Barcelona, Spain: Universitat Barcelona; 2004. p. 1061

[12] Bender R, Schütze M. Materials and Corrosion. 2003;**54**:652

[13] Fähsing D, Rudolphi M, Konrad L, Galetz MC. Oxidation of Metals. 2017;**88**:155

[14] Kumagai M, Shibue K, Kim M-S, Yonemitsu M. Intermetallics. 1996;**4**:557

[15] Taniguchi S. Materials and Corrosion. 1997;**48**:1

[16] Schütze M, Hald M. Material Science Engineering A. 1997;**239-240**:847

[17] Donchev A, Gleeson B, Schütze M. Intermetallics. 2003;**11**:387

[18] Donchev A, Zschau H-E, Schütze M. Mat. High Temperature. 2005;**22**:309

[19] Hindam H, Whittle DP. Oxidation of Metals. 1982;**18**:245

[20] Poirier DR, Geiger GH. Transport Phenomena in Materials Processing. Warrendale, USA: TMS; 1994

[21] Kofstad P. High Temperature Corrosion. London, UK: Elsevier; 1988

http://dx.doi.org/10.5772/intechopen.75696

[22] Computer Software Packages ChemSage and FactSage by GTT-Technologies GmbH, Herzogenrath, Germany

[23] Zschau H-E, Gauthier V, Schumacher G, Dettenwanger F, Schütze M, Baumann H, Bethge K, Graham M. Oxidation of Metals. 2003;**59**:183

[24] Anders A. Handbook of Plasma Immersion Ion Implantation and Deposition. New York, USA: John Wiley & Sons; 2000

IntechOpen
IntechOpen

IntechOpen

IntechOpen